

## Predicting the increase in electron affinity of phenoxy upon fluorination

Connor J. Clarke<sup>a</sup>, Jemma A. Gibbard<sup>a</sup>, William D.G. Brittain<sup>a</sup>, Jan R.R. Verlet<sup>a,b,\*</sup>

<sup>a</sup> Department of Chemistry, Durham University, Durham DH1 3LE, United Kingdom

<sup>b</sup> J. Heyrovský Institute of Physical Chemistry, Czech Academy of Sciences, Dolejškova 3, 18223 Prague, Czech Republic

### ARTICLE INFO

#### Keywords:

Electron affinity  
Anion photoelectron spectroscopy  
Phenoxy radical  
Fluorination  
Fluorine chemistry

### ABSTRACT

The site-specific fluorination of organic compounds can alter their electron affinity, *EA*, which in turn can be used to control their reactivity, physical properties, or binding affinities. Using anion photoelectron spectroscopy, we show that for the multiply fluorinated phenoxy radical, the change in *EA* is predominantly additive per fluorination and can be predicted by the simple formula:  $\Delta EA = \sum_i \Delta EA_i - \Delta EA_C$ , where the numeric index *i* indicates the positions of fluorination. A small cooperative effect,  $\Delta EA_C$ , destabilizes the anion, but this only accounts for 11 % of the total  $\Delta EA$ , in the extreme case of pentafluorophenolate. Our experimental results are consistent with those calculated using density functional theory, demonstrating the suitability of electronic structure calculations in the prediction of fluorination effects, for practical use in the synthetic design of organofluorines.

Fluorinated organic molecules are commonly utilized in medicinal, agricultural, and materials chemistry [1–5]. The fluorine atom has a similar van der Waals' radius to hydrogen but is far more electronegative [6,7], allowing fluorination to influence the electronic structure of a molecule with minimal steric effects. Selective fluorination has been used to tune the chemical properties of compounds, including the electron affinity (*EA*) [8–10]. This has consequences for leaving groups in  $S_N2$  and E2 reactions [11], the electron transport properties of molecular electronics [12–15], and binding within macromolecular environments (e.g. through anion- $\pi$  bonding) [16,17]. Indeed, several synthetic methodologies have been developed that utilize the influence that fluorinated moieties can have on adjacent functional groups [11,18,19]. For example, as schematically shown in Fig. 1, the use of semi- and per-fluorinated phenolic functionality to both generate activated esters and to act as good leaving groups for conjugation chemistry has been widely employed to access novel small molecules [20,21], peptides [22,23], supramolecular architectures [24] and polymers [25,26]. Understanding exactly how selective fluorination tunes the *EA* is therefore a potentially powerful tool in predicting chemical, biological, or physical outcomes and is key to developing structure-function relationships. To this end, in the present study, we use photoelectron spectroscopy to systematically study the effect of selective fluorination on the *EA* of the phenoxy radical to form phenolate, showing that fluorination at the 2-, 3-, and 4-positions of the phenol ring leads to distinct and predictable increases in the *EA*, and that the contributions of each individual substitution are almost purely additive.

The *EA* can be accurately quantified through anion photoelectron spectroscopy [27] and previous measurements have shown that fluorination generally leads to a larger *EA* [10,28–30] due to the electron-withdrawing character of F aiding delocalization of the excess charge in the anion. Recently, the relationship between the *EA* and fluorination has been further explored in fluorophenyl radicals ( $\bullet C_6H_{5-x}F_x$ ). The *EA* was observed to increase linearly with a greater degree of fluorination, site-selective fluorination was noted, and the reactive center on the anion versus the radical was observed to differ [31,32]. In the present study, we focus on the phenoxy radical,  $C_6H_5O\bullet$ , and consider its *EA* upon regioselective fluorination and therefore upon the stability of the phenolate anion. Phenolate is a key component of many biological (and synthetic) chromophores, such as tyrosine and in photoactive proteins [33–35]. Based on considerations of the available resonance Lewis structures of phenolate, the negative charge localizes predominantly on the oxygen atom, as well as the carbon atoms in the 2/6 and 4 positions. One may therefore expect the electronic properties of the phenolate anion to be sensitive to both the position and degree of fluorination.

We probe the effect of fluorination on the *EA* of the phenoxy radical through photoelectron spectroscopy of the phenolate anion ( $PhO^-$ ) and its monofluorinated derivatives: 2-, 3-, and 4-fluorophenolate (2-MFP<sup>-</sup>, 3-MFP<sup>-</sup>, 4-MFP<sup>-</sup>). In order to understand whether the effect of multiple fluorinations is additive, we also studied fluorophenolates with a higher degree of fluorination: (2,3,4)-, (2,4,6)-, and (3,4,5)-trifluorophenolate (2,3,4-TFP<sup>-</sup>, 2,4,6-TFP<sup>-</sup>, 3,4,5-TFP<sup>-</sup>), and the perfluorinated species,

\* Corresponding author at: Department of Chemistry, Durham University, Durham DH1 3LE, United Kingdom.

E-mail address: [j.r.r.verlet@durham.ac.uk](mailto:j.r.r.verlet@durham.ac.uk) (J.R.R. Verlet).

<https://doi.org/10.1016/j.jfluchem.2024.110306>

Received 29 April 2024; Received in revised form 30 May 2024; Accepted 30 May 2024

Available online 4 June 2024

0022-1139/© 2024 The Author(s). Published by Elsevier B.V. This is an open access article under the CC BY license (<http://creativecommons.org/licenses/by/4.0/>).

pentafluorophenolate (PFP<sup>-</sup>). Taken together, composite fluorination effects could therefore be unpacked into their individual contributions.

Photoelectron spectra of PhO<sup>-</sup> and the fluorophenolate anions were acquired with nanosecond laser pulses. The photon energy  $h\nu$  was tuned between the visible and UV ranges to slightly exceed the onset of photoelectron detachment for each anion, enhancing the observed vibrational structure in the spectra (experimental details are given in the Supplementary Information). We first focused on the singly fluorinated species (2-, 3-, and 4-MFP<sup>-</sup>) and their comparison to PhO<sup>-</sup>. The photoelectron spectra are shown in Fig. 2, presented in terms of electron binding energy, defined as  $eBE = h\nu - eKE$ , where  $eKE$  is the electron kinetic energy. The photoelectron spectrum of PhO<sup>-</sup> is well-studied [36–41], and the peak centered at  $eBE = 2.25$  eV (marked with a black arrow) corresponds to the 0–0 transition for direct photodetachment of the ground-state phenolate anion, forming the neutral radical species in its ground electronic state ( $S_0 + h\nu \rightarrow D_0 + e^-$ ). Vibrational structure appears throughout the feature, which has been characterized in earlier high-resolution photoelectron spectroscopic studies [38]. Photoelectron signal on the low- $eBE$  side of the 0–0 transition arises from hot-bands. Our resolution in determining the 0–0 transition is  $\pm 0.02$  eV and is similar for all fluorinated species studied. The 0–0 transition is a direct measurement of the  $EA$  of the corresponding radical.

The 0–0 transition, labeled with colored arrows, is also observed from the three monofluorophenolates, but has shifted to a higher  $eBE$  in each case. This indicates that fluorination indeed increases the  $EA$  of the phenoxy radical, but to a different extent depending on the regiochemistry of fluorination. To ensure the correct identification of the 0–0 transition, complimentary vibronic spectra were computed using density functional theory (DFT), which are shown in the Supplementary Information and demonstrate excellent overall agreement.

From the 3-fluorophenolate spectrum, we find that  $EA_{3\text{-MFP}} = 2.53$  eV compared to the phenoxy radical  $EA_{\text{PhO}} = 2.25$  eV. Therefore, the change in electron affinity associated with fluorination at the 3-position (meta)  $\Delta EA_3 = +0.28$  eV. Of course, this is the same as the 5-position:  $\Delta EA_3 = \Delta EA_5 = \Delta EA_{3/5}$ . Fluorination at the 2/6- (ortho) or at the 4-position (para) also increases the  $EA$  but to a lesser degree, and their influences can be quantified from Fig. 2 as  $\Delta EA_{2/6} = +0.18$  eV and  $\Delta EA_4 = +0.05$  eV, respectively. In each case, the fluorine atom acts as an electron-withdrawing group, aiding delocalization of the excess negative charge in the anion. Substitution in the 3/5-position stabilizes the anion most effectively, consistent with other observations on the

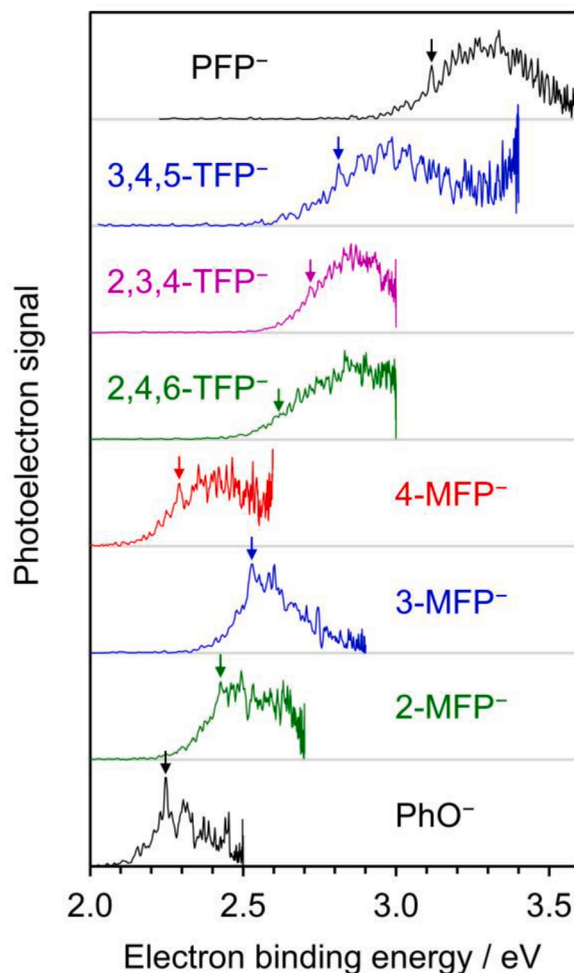


Fig. 2. Photoelectron spectra of phenolate (PhO<sup>-</sup>) and fluorophenolate anions, acquired with nanosecond laser pulses in the UV–vis region. The three possible MFP anions were studied, labelled by their fluorination sites and discriminated by color: 2 (green), 3 (blue), and 4 (red). Three TFP anions were also studied: 2,4,6 (green), 2,3,4 (purple) and 3,4,5 (blue); as well as PFP<sup>-</sup>. Vertical arrows indicate the position of the extracted electron affinity ( $EA$ ) for each species.

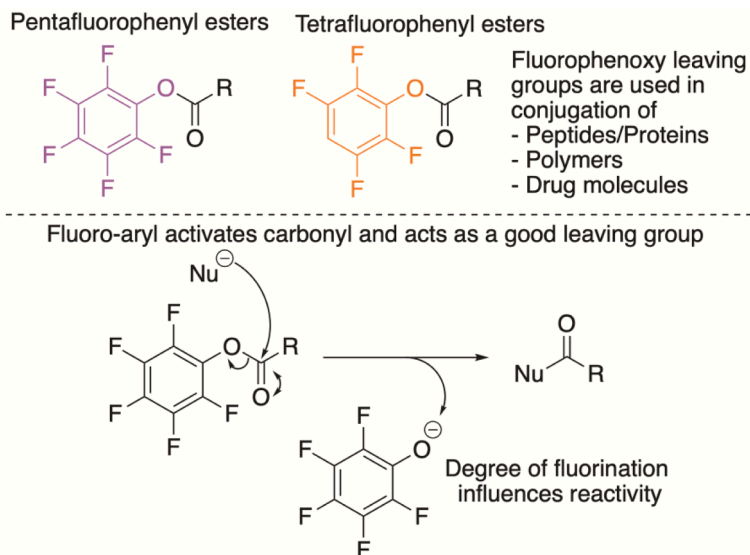


Fig. 1. Schematic showing the importance of fluorinated phenolate anions as part of fluorophenyl esters. The phenolate anion capacity as a good leaving group depends on the electron affinity of its radical.

substituted phenolate (and halobenzy) anions [42–45].

Fig. 2 also displays the photoelectron spectra acquired from the tri- and penta-fluorophenolate anions. It is apparent that the *EA* continues to increase with an increasing degree of fluorination. The less resolved vibrational structure exhibited in these species (especially 2,4,6-TFP<sup>−</sup>), as well as the presence of hot-bands, made determination of the 0–0 transition energy less obvious. Nevertheless, confident assignment was still possible with the assistance of computations (see Supplementary Information). The successive increases in *EA* with fluorination culminates in  $EA_{\text{PFP}} = 3.12$  eV for PFP, which is nearly 1 eV higher than the non-fluorinated phenoxy radical. We noted that low-energy electrons ( $eBE \sim h\nu$ ) are observed in the photoelectron spectra of the TFPs, particularly in 3,4,5-TFP<sup>−</sup>. These electrons arise from thermionic emission processes, suggesting that an excited state of the anion is being populated at the applied photon energies [46–48]. The excitation energy has been shown to depend on the degree of fluorination in earlier photoelectron spectroscopic studies on the 3,5-difluorophenolate anion [49], and the role of site-specific effects will be the topic of a future study where such optical properties can be systematically tuned.

From the results of the monofluorophenolate anions, it was shown that fluorination at the 3- or 5-position (meta) has a more stabilizing effect on the phenolate anion than does 2- or 6-fluorination (ortho). Comparison between the *EA* of 2,4,6-TFP<sup>−</sup> and 3,4,5-TFP<sup>−</sup> further corroborates this finding. The change in electron affinity associated with (2,4,6) fluorination is  $\Delta EA_{246} = +0.38$  eV, whereas (3,4,5) fluorination exerts a larger effect of  $\Delta EA_{345} = +0.57$  eV. As expected, (2,3,4) fluorination had a medial effect of  $\Delta EA_{234} = +0.47$  eV. The resulting trends suggest that the effects of each individual fluorination may be independent of any others on the aromatic ring. To investigate further, we compared  $\Delta EA$  values associated with the multiply fluorinated species to the sum of the individual values associated with the corresponding MFP molecules,  $\Delta EA_i$ , where index *i* labels the position of monofluorination. For example,  $\Delta EA_{234}$  was compared to  $\Delta EA_{2/6} + \Delta EA_{3/5} + \Delta EA_4$ . The comparisons are displayed as a bar-chart in Fig. 3, where the measured increase in *EA* associated with the multiple fluorinations (i.e.,  $\Delta EA$  of the TFP<sup>−</sup> and PFP<sup>−</sup> anions) is denoted  $\Delta EA^*$ . Fig. 3 shows that, in each case, the sum of the individual  $\Delta EA_i$  that make up the tri- and penta-fluorinated phenoxy radicals account for most its  $\Delta EA^*$ , demonstrating that the increase in *EA* due to fluorination of the aromatic ring is mostly additive. Nevertheless, a small additional contribution arises which is a

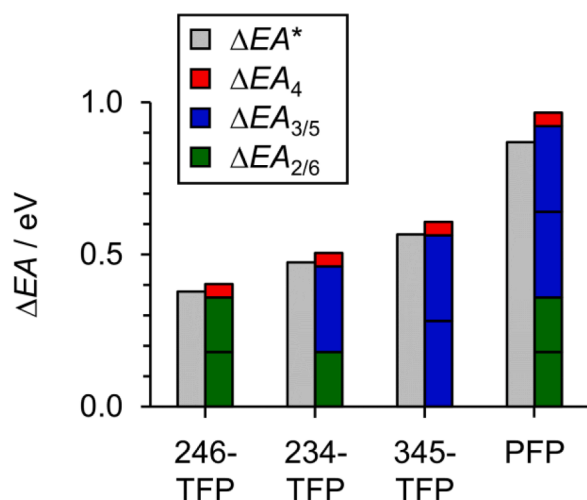


Fig. 3. The experimentally determined difference in electron affinity (*EA*) between phenoxy (PhO) and the multiply fluorinated fluorophenoxy species,  $\Delta EA^*$  (gray). These are compared to the *EA* differences between PhO and the MFP species which contain the corresponding fluorination sites, which is denoted  $\Delta EA_i$  where the index *i* indicates the fluorination site (2/6 in green, 3/5 in blue, or 4 in red).

counteracting contribution that lowers the *EA* (i.e., a negative  $\Delta EA$  contribution).

For the three TFP<sup>−</sup> species, the measured  $\Delta EA^*$  is 6–7 % lower than the summed  $\Delta EA_i$  contributions. The origin of this non-additive destabilizing effect can be rationalized as follows. In going from phenolate to monofluorophenolate anions, the electron density on the aromatic ring is withdrawn by the electronegative fluorine atom. The two additional fluorine atoms present in the TFP<sup>−</sup> anions also act to withdraw the electron density, but there is less partial negative charge to be withdrawn from the ring, and therefore further fluorination results in slightly less stabilization of the anion per additional F atom introduced. The effect is further exacerbated in PFP<sup>−</sup>, where five fluorine atoms act to simultaneously withdraw the electron density, and therefore the  $\Delta EA^*$  of PFP<sup>−</sup> shows the greatest deviation to the summed  $\Delta EA_i$  contributions (11 %). This cooperative effect,  $\Delta EA_C$ , is small compared to the total stabilization that each fluorine atom provides and, to a first approximation, it is sensible to consider the stabilization arising in the poly-fluorinated phenolate species to the additive contributions from component fluorinations. Within this approximation, the effect of fluorination on the electron affinity of the phenoxy radical is shown pictorially in Fig. 4. Our findings can be summarized by the following equation:  $\Delta EA^* = \sum_i \Delta EA_i - \Delta EA_C$ , where index *i* runs over each fluorinated site in a multiply fluorinated phenoxy radical.

The *EA* of each fluorophenoxy radical was also calculated using DFT applied at the B3LYP/aug-cc-pVTZ level (details in Supplementary Information) [50,51]. All the calculated *EA* values were found to be in excellent agreement with the experiments, lying between 0.03 and 0.05 eV lower in energy than the experimentally determined values (see Table S1 in the Supplementary Information). The effects of fluorination on the *EA* are captured very well within the DFT calculations. Therefore, one can have confidence in using computational chemistry to guide chemical design, at least for phenolate anions. A comparison between the calculated  $\Delta EA^*$  and sum of calculated individual contributions,  $\Delta EA_i$ , is also included in the Supplementary Information, and shows good agreement with the results displayed in Fig. 3. In addition, natural population analysis was applied to probe further into the cooperative effect  $\Delta EA_C$ , described above. As expected, each additional fluorine atom acts to withdraw electron density from the aromatic ring. However, on average, the natural partial charge associated with the fluorine atoms becomes less negative with an increasing degree of fluorination. This indicates that the electron-withdrawing capability of each individual fluorine atom is reduced when there are other fluorine atoms on the ring, consistent with our intuition-based explanation of the cooperative effect.

In conclusion, we demonstrate that the electron binding properties of the phenolate anion are sensitive to the degree and position of fluorination. Moreover, the effect on the electron affinity from multiple fluorinations can be treated as independent from one another, with the caveat being that there is a small reduction in the effectiveness of anion

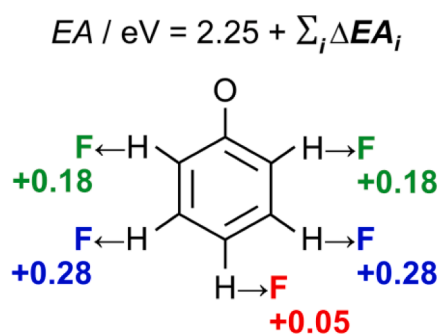


Fig. 4. Schematic showing the approximate effect of fluorination in position *i* on the electron affinity (*EA*) of the phenoxy radical. In this approximation, the small cooperative effect has been ignored.

stabilization per incrementally added F atom. In the perfluorinated phenolate, the change in *EA* predicted from the independent treatment differs to the measured value by only 11 %. Electronic structure calculations (DFT) were found to replicate the stabilizing effects of fluorination. Taken together, this study demonstrates the predictability in fluorination effects on the *EA* of a small aromatic molecule and emphasizes the tunability of selective fluorination. It offers clear and straightforward design routes to synthetically increase the stability of anions through fluorination for applications in various branches of chemistry including synthetic methodology, materials chemistry, and bio/medical chemistry. For example, with reference to Fig. 1, the  $S_{N2}$  rate can be increased by virtue of the more stable phenolate anion upon fluorination, offering a direct route to controlling chemical reactivity. In extreme cases, fluorination has also been predicted to lead to the formation of organic superhalogens, where the *EA* is larger than halogen atoms [8,9].

### CRedit authorship contribution statement

**Connor J. Clarke:** Writing – review & editing, Writing – original draft, Methodology, Formal analysis, Data curation. **Jemma A. Gibbard:** Writing – review & editing, Data curation, Conceptualization. **William D.G. Brittain:** Writing – review & editing, Validation. **Jan R.R. Verlet:** Writing – review & editing, Supervision, Funding acquisition, Conceptualization.

### Declaration of competing interest

The authors declare that they have no conflict of interest.

### Data availability

The data is available at DOI:10.5281/zenodo.10939911.

### Acknowledgments

Jemma A. Gibbard is grateful for support from a Royal Society University Research Fellowship (URF\R1\221140) and Connor J. Clarke for a Durham Doctoral Scholarship. Jan R. R. Verlet is grateful for funding from OP JAK project No. CZ.02.01.01/00/22\_008/0004649 (QUEENTEC) and the Engineering and Physical Sciences Research Council (grant number EP/V007971/1).

### Supplementary materials

Supplementary material associated with this article can be found, in the online version, at doi:10.1016/j.jfluchem.2024.110306.

### References

- [1] K. Müller, C. Faeh, F. Diederich, *Science* 317 (2007) 1881–1886.
- [2] S. Purser, P.R. Moore, S. Swallow, V. Gouverneur, *Chem. Soc. Rev.* 37 (2008) 320–330.
- [3] G. Theodoridis, in: A. Tressaud (Ed.), *Advances in Fluorine Science*, 2, Elsevier, 2006, pp. 121–175. doi:10.1016/S1872-0358(06)02004-5.
- [4] Y. Ogawa, E. Tokunaga, O. Kobayashi, K. Hirai, N. Shibata, *iScience* 23 (2020) 101467.
- [5] N. Leclerc, P. Chávez, O.A. Ibraikulov, T. Heiser, P. Lévêque, *Polymers* 8 (2016) 11.
- [6] A. Bondi, *J. Phys. Chem.* 68 (1964) 441–451.
- [7] D.R. Lide (Ed.), *CRC Handbook of Chemistry and Physics* 85 (2004).
- [8] B.Z. Child, S. Giri, S. Gronert, P. Jena, *Chem. Eur. J.* 20 (2014) 4736–4745.
- [9] S. Giri, B.Z. Child, P. Jena, *ChemPhysChem* 15 (2014) 2903–2908.
- [10] J. Warneke, G.-L. Hou, E. Aprà, C. Jenne, Z. Yang, Z. Qin, K. Kowalski, X.-B. Wang, S.S. Xantheas, *J. Am. Chem. Soc.* 139 (2017) 14749–14756.
- [11] C. Ni, J. Hu, *Chem. Soc. Rev.* 45 (2016) 5441–5454.
- [12] S. Dai, F. Zhao, Q. Zhang, T.-K. Lau, T. Li, K. Liu, Q. Ling, C. Wang, X. Lu, W. You, X. Zhan, *J. Am. Chem. Soc.* 139 (2017) 1336–1343.
- [13] W. Zhao, S. Li, H. Yao, S. Zhang, Y. Zhang, B. Yang, J. Hou, *J. Am. Chem. Soc.* 139 (2017) 7148–7151.
- [14] K. Feng, X. Zhang, Z. Wu, Y. Shi, M. Su, K. Yang, Y. Wang, H. Sun, J. Min, Y. Zhang, X. Cheng, H.Y. Woo, X. Guo, *ACS Appl. Mater. Interfaces* 11 (2019) 35924–35934.
- [15] N.N. Tri, Y.M. Hailu, L. Van Duong, M.T. Nguyen, *J. Fluor. Chem.* 240 (2020) 109665.
- [16] C.S. Anstöter, J.P. Rogers, J.R.R. Verlet, *J. Am. Chem. Soc.* 141 (2019) 6132–6135.
- [17] D.-X. Wang, M.-X. Wang, *Acc. Chem. Res.* 53 (2020) 1364–1380.
- [18] E. Bogdan, G. Compain, L. Mtashobya, J.-Y. Le Questel, F. Besseau, N. Galland, B. Linclau, J. Graton, *Chem. Eur. J.* 21 (2015) 11462–11474.
- [19] W.D.G. Brittain, S.L. Cobb, *J. Org. Chem.* 85 (2020) 6862–6871.
- [20] B.G. Avitabile, C.A. Smith, D.B. Judd, *Org. Lett.* 7 (2005) 843–846.
- [21] H. Li, Y. Hou, C. Liu, Z. Lai, L. Ning, R. Szostak, M. Szostak, *J. An, Org. Lett.* 22 (2020) 1249–1253.
- [22] M. Meldal, K.J. Jensen, *J. Chem. Soc., Chem. Commun.* (1990) 483–485.
- [23] A.T. Ślósarczyk, R. Ramapanicker, T. Norberg, L. Baltzer, *RSC Adv.* 2 (2012) 908–914.
- [24] M. Rémy, I. Nierengarten, B. Park, M. Holler, U. Hahn, J.-F. Nierengarten, *Chem. Eur. J.* 27 (2021) 8492–8499.
- [25] P.J. Roth, K.T. Wiss, R. Zentel, P. Theato, *Macromolecules* 41 (2008) 8513–8519.
- [26] N.K. Singha, M.I. Gibson, B.P. Koiry, M. Danial, H.-A. Klok, *Biomacromolecules* 12 (2011) 2908–2913.
- [27] M.L. Weichman, D.M. Neumark, *Annu. Rev. Phys. Chem.* 69 (2018) 101–124.
- [28] I.N. Ioffe, S.M. Avdoshenko, O.V. Boltalina, L.N. Sidorov, K. Berndt, J.M. Weber, *Int. J. Mass Spectrom.* 243 (2005) 223–230.
- [29] T. Masubuchi, Y. Sugawara, A. Nakajima, *J. Chem. Phys.* 145 (2016) 244306.
- [30] J.L. Woodhouse, A. Henley, R. Lewin, J.M. Ward, H.C. Hailes, A.V. Bochenkova, H. H. Fielding, *Phys. Chem. Chem. Phys.* 23 (2021) 19911–19922.
- [31] C.J. McGee, K.R. McGinnis, C.C. Jarrold, *J. Phys. Chem. A* 127 (2023) 7264–7273.
- [32] K.R. McGinnis, C.J. McGee, C.C. Jarrold, *J. Am. Chem. Soc.* 146 (2024) 7063–7075.
- [33] D.S. Larsen, M. Vengris, I.H.M. van Stokkum, M.A. van der Horst, F.L. de Weerd, K. J. Hellingwerf, R. van Grondelle, *Biophys. J.* 86 (2004) 2538–2550.
- [34] C.S. Anstöter, B.F.E. Curchod, J.R.R. Verlet, *Nat. Commun.* 11 (2020) 2827.
- [35] C.S. Anstöter, J.R.R. Verlet, *Acc. Chem. Res.* 55 (2022) 1205–1213.
- [36] R.F. Gunion, M.K. Gilles, M.L. Polak, W.C. Lineberger, *Int. J. Mass Spectrom. Ion Processes* 117 (1992) 601–620.
- [37] A.R. McKay, M.E. Sanz, C.R.S. Mooney, R.S. Minns, E.M. Gill, H.H. Fielding, *Rev. Sci. Instrum.* 81 (2010) 123101.
- [38] J.B. Kim, T.I. Yacovitch, C. Hock, D.M. Neumark, *Phys. Chem. Chem. Phys.* 13 (2011) 17378–17383.
- [39] H.-T. Liu, C.-G. Ning, D.-L. Huang, P.D. Dau, L.-S. Wang, *Angew. Chem.* 125 (2013) 9146–9149.
- [40] A.M. Buytendyk, J.D. Graham, K.D. Collins, K.H. Bowen, C.-H. Wu, J.I. Wu, *Phys. Chem. Chem. Phys.* 17 (2015) 25109–25113.
- [41] M. Elena Castellani, C.S. Anstöter, J.R.R. Verlet, *Phys. Chem. Chem. Phys.* 21 (2019) 24286–24290.
- [42] J.B. Kim, P.G. Wenthold, W.C. Lineberger, *J. Phys. Chem. A* 103 (1999) 10833–10841.
- [43] D.J. Nelson, W.K. Gichuhi, E.M. Miller, J.H. Lehman, W.C. Lineberger, *J. Chem. Phys.* 146 (2017) 074302.
- [44] D.J. Nelson, W.K. Gichuhi, C.M. Nichols, V.M. Bierbaum, W.C. Lineberger, J. H. Lehman, *Phys. Chem. Chem. Phys.* 20 (2018) 25203–25216.
- [45] D.H. Kang, J. Kim, H.J. Eun, S.K. Kim, *J. Am. Chem. Soc.* 144 (2022) 16077–16085.
- [46] D.A. Horke, Q. Li, L. Blancafort, J.R.R. Verlet, *Nat. Chem.* 5 (2013) 711–717.
- [47] C.S. Anstöter, J.N. Bull, J.R.R. Verlet, *Int. Rev. Phys. Chem.* 35 (2016) 509–538.
- [48] G.A. Cooper, C.J. Clarke, J.R.R. Verlet, *J. Am. Chem. Soc.* 145 (2023) 1319–1326.
- [49] J.L. Woodhouse, A. Henley, M.A. Parkes, H.H. Fielding, *J. Phys. Chem. A* 123 (2019) 2709–2718.
- [50] R.A. Kendall, T.H. Dunning Jr., R.J. Harrison, *J. Chem. Phys.* 96 (1992) 6796–6806.
- [51] P.J. Stephens, F.J. Devlin, C.F. Chabalowski, M.J. Frisch, *J. Phys. Chem.* 98 (1994) 11623–11627.